


Influence of goethite on the Transportable Moisture Limit of iron ore fines

Raphael Lessa de Paula¹ Rodrigo Fina Ferreira^{2*} Rosa Malena Fernandes Lima³ 

Abstract

Iron ore is a major seaborne commodity, and its transport is regulated by the International Maritime Organization (IMO). To prevent excess moisture related accidents, the IMO sets a Transportable Moisture Limit (TML) for iron ore fines, which is the moisture content at which the material reaches 80% saturation, determined through laboratory tests. Recent research has shown that TML is influenced by a variety of factors, including particle size distribution, mineralogical composition, and solids density. However, the influence of goethite on TML has not been fully explored, and this was the subject of the present work. The results show that goethite content is positively correlated with TML. Samples with higher goethite content exhibited reduced compaction, leading to larger void volumes within the compacted material. This reduced packing density likely contributes to the higher TML observed. Goethite's lower solids density is also a relevant contributing factor. Further research is needed to understand the specific mechanisms underlying the differences in compaction behaviour and its impact on different iron ore compositions.

Keywords: Iron ore fines; Transportable Moisture Limit; Goethite.

Influência da goethita no Limite de Umidade Transportável de finos de minério de ferro

Resumo

O minério de ferro é uma das principais commodities transportadas via marítima e seu transporte é regulamentado pela Organização Marítima Internacional (IMO). Para prevenir acidentes relacionados a excesso de umidade da carga, a IMO estabelece um Limite de Umidade Transportável (TML) para os finos de minério de ferro, que corresponde à umidade na qual o material atinge 80% de saturação, determinada por testes laboratoriais. Pesquisas recentes demonstraram que o TML é influenciado por diversos fatores, incluindo granulometria, composição mineralógica e densidade dos sólidos. No entanto, a influência da goethita no TML não foi explorada a fundo, tendo sido o objeto de estudo do presente trabalho. Os resultados mostraram que o teor de goethita está positivamente correlacionado com o TML. Amostras com maior participação de goethita apresentaram menor compactação, levando a um maior volume de vazios no material compactado. Esta menor densidade de empacotamento contribui para o TML mais elevado. A menor densidade dos sólidos da goethita também é um fator contribuinte relevante. Pesquisas adicionais são necessárias para entender os mecanismos específicos relacionados às diferenças no comportamento frente à compactação e seu impacto em diferentes composições de minério de ferro.

Palavras-chave: Finos de minério de ferro; Limite de Umidade Transportável; Goethita.

1 Introduction

International Maritime Organization (IMO) regulations stipulate that cargoes vulnerable to excess moisture related risks shall be loaded and transported below the Transportable Moisture Limit (TML), determined by laboratory tests. This study focuses on iron ore fines, for which the modified Proctor

Fagerberg test for iron ore fines (PFD80 test) [1] defines TML as the moisture content for 80% saturation after compacting the ore under a 27.59 kJ/m³ compaction energy. This definition suggests a direct link between TML and the ore's void volume, a relationship also emphasized by Ferreira et al. [2], who

¹Centro de Pesquisas Tecnológicas, Vale S/A, Nova Lima, MG, Brasil.

²Desenvolvimento de Processo Mineral, Vale S/A, Nova Lima, MG, Brasil.

³Departamento de Engenharia de Minas, Universidade Federal de Ouro Preto, UFOP, Ouro Preto, MG, Brasil.

*Corresponding author: rodrigo.fina@vale.com



demonstrated the importance of void ratio in understanding TML variations. This highlights that TML depends on the specific characteristics of the tested material.

While the TML plays a crucial role in the safe transport of mineral cargoes, research on its relationship with ore characteristics remains limited. Ferreira [3] developed models for predicting TML and identified relationships between the parameter and some ore features. The author concluded that TML is a multi-dependent variable, influenced by particle size distribution, mineralogical composition, solids density, and other properties. Ferreira and Lima [4] explored the effect of particle size distribution, revealing its impact on TML through void volume variations. The authors pointed out that the resulting TML of mixtures of different ores may not be the result of the weighted average of the individual components' TML. Furthermore, they identified a useful inverse relationship between TML and the coefficient of uniformity. In a later study [5], the same authors experimentally investigated the relationship between TML and solids density. Their findings confirmed the theoretical prediction of an inverse relationship: higher density solids corresponded to lower TML values. These findings underscore the complexity of TML, compelling further exploration of its dependence on diverse ore characteristics to ensure safe and efficient mineral transportation.

China's growing demand for iron ore in recent decades has significantly inflated prices, making previously marginal Brazilian ores, like compact and goethitic itabirites, economically viable to mine and process [6]. The International Maritime Solid Bulk Cargoes Code (IMSBC Code), established by the IMO, provides safety guidelines for transporting solid bulk cargoes like iron ore fines and classifies them in three groups [1]: Group A: cargoes which may liquefy; Group B: cargoes which possess a chemical hazard; Group C: cargoes which are neither liable to liquefy nor to possess chemical hazards. Under this system, iron ore fines with a goethite content exceeding 35% fall into Group C, indicating no liquefaction risk, and those with less than 35% goethite are categorized as Group A cargoes, requiring TML determination. This regulatory framework draws on research conducted by the IMO's Iron Ore Fines Technical Working Group (IOFTWG) [7-11], which adapted the Proctor/Fagerberg test for iron ore fines. Given the increasing prevalence of goethite in iron ore products, understanding how variations between 0-35% in goethite content influence TML becomes crucial. However, no study in the literature has explored this specific relationship. Therefore, this research aims to address the existing gap in knowledge by investigating the impact of goethite content on the TML of iron ore fines as defined by the PFD80 method.

2 Materials and methods

The influence of goethite content on the TML of iron ore fines was investigated employing a Simplex Lattice design of degree 3 using Minitab™ 21.1 software [12] was employed. This design allows for creating mixtures with

controllable compositions, ideal for studying how individual components impact a target property.

Two iron ore fine samples with 150 kg each were used as starting points: sinter feed 1 (SF1) with low goethite content and sinter feed 2 (SF2) with high goethite content. The design yielded seven sub-samples with varying proportions of SF1 and SF2: SF1 (100% SF1), SF2 (100% SF2), MX1 (25% SF1 - 75% SF2), MX2 (33% SF1 - 67% SF2), MX3 (50% SF1 - 50% SF2), MX4 (67% SF1 - 33% SF2), and MX5 (75% SF1 - 25% SF2).

2.1 Physical characterization

Particle size distribution of both SF1 and SF2 was determined by sequential wet sieving (19.0-0.045 mm) using laboratory sieves and laser diffraction (LALLS - Low Angle Laser Light Scattering) for the <0.045 mm fraction with a Mastersizer 2000 from Malvern Instruments. Solids density (ρ) was measured using a Pentapycnometer (Quantachrome) following ASTM D5550-14 guidelines [13]. Pore size distribution was determined through nitrogen adsorption using the BJH (Barrett-Joyner-Halenda) technique on a Nova 1000e apparatus (Quantachrome). Finally, the particle size distributions, solids densities, and mean pore sizes of the resulting mixture samples were calculated based on the proportions of SF1 and SF2 in each mixture.

2.2 Chemical characterization and Loss on Ignition (LOI)

Chemical analyses of SF1 and SF2 were conducted via X-ray fluorescence using a Rigaku Simultix 12 spectrometer, in accordance with ISO 9516-1:2003 standards [14]. Loss on Ignition (LOI) was determined by the weight loss after calcination at 1,000 °C for 1 hour in a muffle furnace. Based on these analyses, the chemical composition and LOI of the mixtures were calculated, considering the proportions of SF1 and SF2 in each mixture.

2.3 Mineralogical characterization

X-ray powder diffraction analysis with a PANalytical Empyrean diffractometer (Co tube, 1.789 Å, 40 kV, 40 mA) revealed the mineralogical composition of the samples. XRDML database was used from the ICDD 2011 (v2.1102) to interpret the obtained diffractograms. Based on these analyses, the Rietveld method with HighScore Plus (v3.0e) software was employed for semi-quantitative analysis of mineral phases. Finally, the mineralogical composition of the mixtures of SF1 and SF2 was calculated, taking into consideration the proportions of the samples in each mixture.

2.4 Modified Proctor/Fagerberg Test (PFD80)

The Transportable Moisture Limit (TML) of the samples and mixtures was determined using the Modified

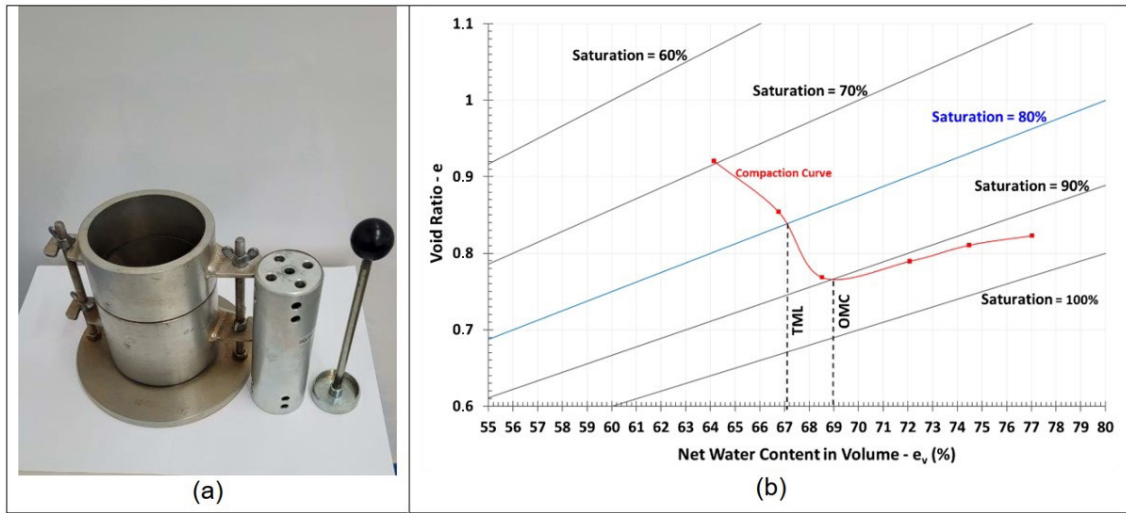


Figure 1. (a) PFD80 test apparatus (mould and hammer); and an example of PFD80 compaction curve (b).

Proctor/Fagerberg Test for Iron Ore Fines (PFD80), following the IMSBC Code guidelines [1]. Five layers of the sample are added and compacted in a cylindrical mould using a hammer (150 g, 50 mm diameter, 150 mm drop) through a guiding tube (Figure 1a). For each moisture content, void ratio (e), net water content (e_v), and degree of saturation (S) are calculated (Equations 1-3). This data is plotted as a graph of void ratio versus net water content, including iso-saturation lines that represent constant saturation degrees (Figure 1b). The TML value is then determined at the intersection point of the compaction curve with the 80% saturation line, as illustrated in Figure 1b, being calculated by Equation 4.

$$e = \frac{V_v}{V_s} \quad (1)$$

$$e_v = \frac{V_w}{V_s} \times 100\% \quad (2)$$

$$S = \frac{e_v}{e} \quad (3)$$

$$TML = \frac{100e_v}{100d + e_v} \quad (4)$$

where d is the solids density, V_v is the void volume, V_w is the volume of water, V_s is the volume occupied by the solids and S is the degree of saturation.

2.5 Data processing

All characterizations and tests were conducted in duplicate, and the average values were used for further analysis. The open-source software R [15] was used for data processing.

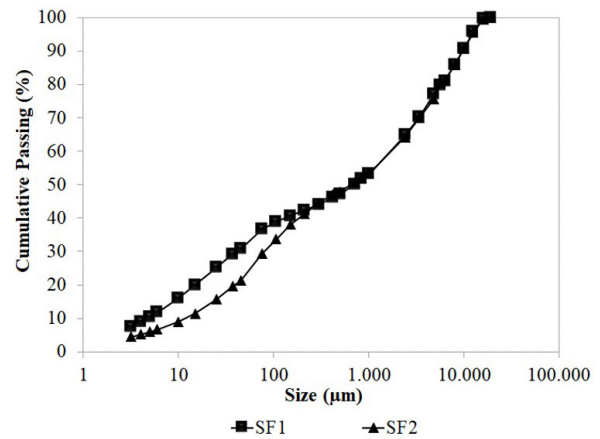


Figure 2. Particle size distribution curves of samples SF1 and SF2.

3 Results and discussion

3.1 Physical properties of the samples

Figure 2 reveals that the iron ore fines in SF1 and SF2 exhibit similar particle size distributions up to 150 μm, diverging in the finer fractions. SF1 displays a finer distribution, with 15.7% of particles smaller than 10 μm compared to 8.6% for SF2. This difference in the finer fractions may be relevant to coefficient of uniformity, which influences the TML, according to Ferreira e Lima [4]. This connection will be further explored later.

Table 1 summarizes the solids density, pore volume (Pore V), pore diameter (Pore D), D_{60} , D_{10} , and coefficient of uniformity ($C_u = D_{60}/D_{10}$) of SF1, SF2, and their mixtures. SF1's average pore size (13.20 nm) surpasses that of SF2 (9.10 nm) by ~31.1%, mirroring the 50% higher total micropore volume. Both C_u and D_{10} follow expected trends:

SF1's higher C_u reflects its wider particle size distribution. In the mixtures, C_u , D_{60} , and D_{10} progressively shift according to the SF1 proportion, as expected.

3.2 Chemical and mineralogical characterization

Table 2 summarizes the chemical composition and LOI for SF1 and SF2. Notably, iron contents remain comparable, while SF2 exhibits higher LOI compared to SF1. Higher LOI values typically indicate greater goethite content.

Table 3 presents the semi-quantitative mineralogical composition.

Analyzing Tables 2 and 3 reveals the higher LOI in SF2 (6.12%) directly aligns with its greater goethite content

(53.40%) compared to SF1 (10.70%). Despite three samples exceeding the 35% goethite threshold for Group C exemption, eliminating TML requirements in practice, the diverse range of goethite content remained crucial for this study. Higher SiO_2 in SF1 likely reflects more quartz. Finally, the higher solids density of SF1 (Table 1) can be attributed to its greater hematite proportion ($d = 5.26 \text{ g/cm}^3$) compared to SF2's higher goethite content ($d = 4.37 \text{ g/cm}^3$) [16].

3.3 Modified Proctor/Fagerberg test (PFD80) TML results

Table 4 and Figure 3 present the average TML values of the samples as a function of the mass proportion of the

Table 1. Physical properties of the samples

Sample	Solids Density d (g/cm^3)	Pore V (cm^3/g)	Pore D (nm)	D_{60} (μm)	D_{10} (μm)	C_u
SF1	4.34	0.024	13.20	1.888	5	387
SF2	4.11	0.012	9.10	1.952	13	151
MX1	4.16	0.015	10.13	1.935	9	205
MX2	4.18	0.016	10.45	1.930	9	222
MX3	4.22	0.018	11.15	1.919	7	262
MX4	4.25	0.020	11.85	1.908	6	307
MX5	4.27	0.021	12.18	1.903	6	327

Table 2. Chemical composition and loss on ignition

Sample	%Fe	% SiO_2	% Al_2O_3	%Mn	%LOI
SF1	56.46	15.58	1.76	0.07	1.94
SF2	56.66	11.71	0.95	0.19	6.12
MX1	56.61	12.68	1.15	0.16	5.08
MX2	56.59	12.99	1.22	0.15	4.74
MX3	56.56	13.65	1.36	0.13	4.03
MX4	56.53	14.30	1.49	0.11	3.32
MX5	56.51	14.61	1.56	0.10	2.99

Table 3. Mineralogical composition

Sample	%Hematite	%Goethite	%Magnetite	%Quartz	%Kaolinite	%Gibbsite
SF1	68.50	10.70	0.60	18.50	1.40	0.30
SF2	32.50	53.40	1.70	11.30	0.00	1.10
MX1	41.50	42.73	1.43	13.10	0.35	0.90
MX2	44.38	39.31	1.34	13.68	0.46	0.84
MX3	50.50	32.05	1.15	14.90	0.70	0.70
MX4	56.62	24.79	0.96	15.12	0.94	0.56
MX5	59.50	21.38	0.88	16.70	1.05	0.50

samples SF1 and SF2. It is evident that there was an increase in the TML value with the rising mass proportion of sample SF2 (53.4% goethite), following a linear trend. Table 4 also present the average void ratio obtained at the TML in the compaction curve (e_{TML}), indicating the compaction level of each sample.

Figure 4 presents a correlogram visually revealing the relationships between TML and various physical, chemical, and mineralogical properties of the samples. Highlighted by histograms, scatter plots, and Pearson correlation coefficients (ranging from -1 to +1), the figure clearly shows strong correlations, with asterisks indicating statistical significance levels (***) corresponds to $p < 0.001$).

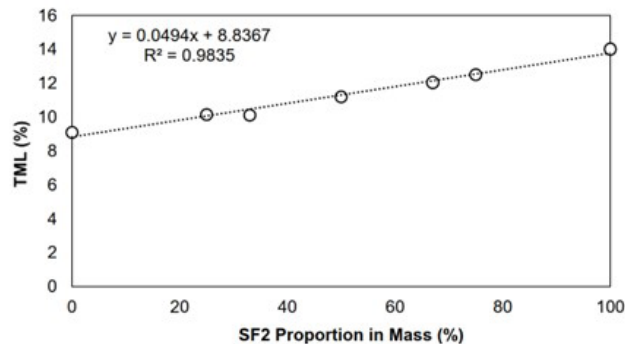


Figure 3. TML as a function of the mass proportion of sample SF2.

TML exhibits a robust positive correlation with goethite proportion and LOI content (as expected due to its link with goethite), while inversely relating to solids density, pore volume (Pore V), and diameter (Pore D). Aligning with previous findings [4], TML and C_u also present an inverse correlation. However, a question arises: could the higher TML in SF1 be entirely explained by its lower goethite content, or might the interplay of goethite content and particle size distribution (reflected by C_u) contribute to this difference? Further investigation into this interaction would be valuable for a deeper understanding of the observed behavior.

To address this question, a targeted granulometric cut was performed on sample SF2 at 2.0 mm, followed by reconstitution to match approximately the same C_u of sample SF1, forming a new sample to be tested (SF2b). This effectively isolated the influence of particle size distribution. Figure 5 compares the adjusted size distribution of SF2b with those of SF1 and SF2. Notably, SF2b exhibits a coefficient of uniformity (393) closely aligning with SF1 (385).

Table 5 reveal that the granulometric modification minimally impacted SF2b chemical and mineralogical compositions. Its chemical analysis, LOI, and mineralogical composition remain virtually identical to those of SF2. This consistency confirms the effectiveness of the intervention in isolating the influence of size distribution on TML, while minimizing compositional alterations.

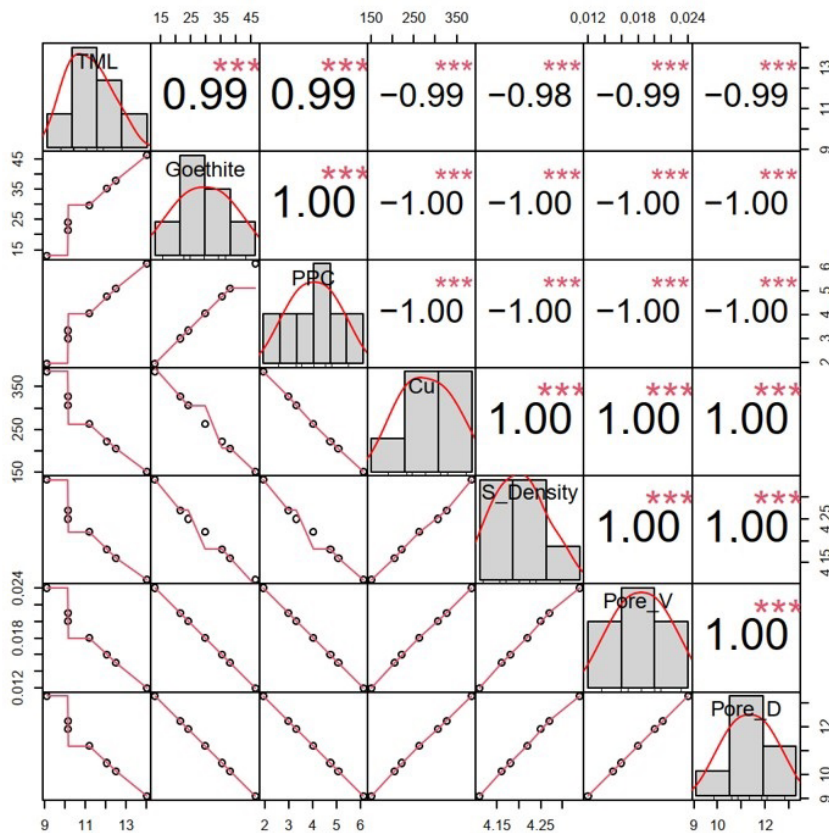


Figure 4. Correlogram between TML and the samples characteristics.

Key data from Table 6 highlight the adjustments made to SF2b. A TML of 13.72% was obtained for sample SF2b, which was marginally lower than the value recorded for sample SF2 (14.03%), aligning with the expected negative C_u -TML trend, but it remains higher than SF1 (9.1%). This suggests that mineralogical variation, primarily goethite content, is the primary determinant of TML.

Two main factors may drive the goethite-TML relationship: porosity and solids density. A higher volume of voids within the ore tends to correlate with higher TML [2]. However, contrary to expectations, a negative relationship between TML and pore features was obtained in this study. This suggests that the contribution of goethite to the increase in TML is not primarily due to a greater porosity. In fact, goethite-rich SF2 exhibits lower porosity than hematite-rich SF1. This observation does not imply a general negative relationship between particle porosity and TML. Instead, it is specific to the tested samples, where the goethite-rich sample displays lower porosity compared to the hematite-rich sample, and other characteristics exert a greater influence on void volume. Regarding solids density, as discussed by Ferreira and Lima [5], for a same void ratio at 80% saturation, the TML value decreases as the solids density increases. This trend was confirmed in this study, as shown in the correlogram in Figure 4. Therefore, the lower solids density of the goethite-rich samples contributes to their higher TMLs.

Furthermore, SF2 and SF2b compact less than SF1 as shown by the void ratio values in Table 4, resulting in higher void volume and consequently, higher TML. While other properties like cohesiveness, particle friction and solid-water relationship likely influence compaction and deserve further investigation, these findings highlight the combined influence of solids density and compaction behaviour in the goethite-TML relationship.

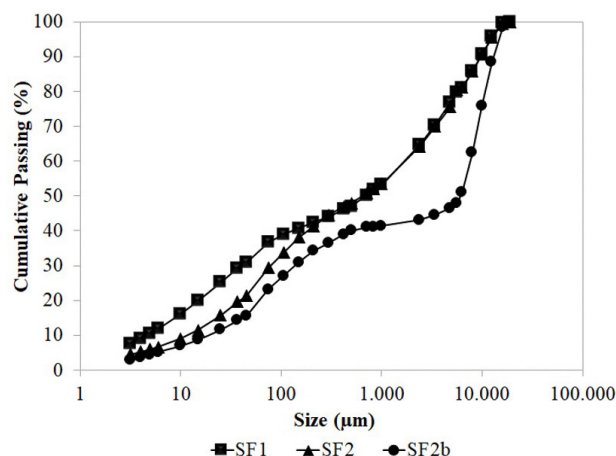


Figure 5. Particle size distribution of samples SF1, SF2 and SF2b.

Table 4. TML results

Sample	Composition	TML (%)	e_{TML}
SF1	100% SF1	9.10	0.547
SF2	100% SF2	14.03	0.836
MX1	25% SF1 + 75% SF2	12.51	0.749
MX2	33% SF1 + 67% SF2	12.04	0.715
MX3	50% SF1 + 50% SF2	11.20	0.666
MX4	67% SF1 + 33% SF2	10.13	0.610
MX5	75% SF1 + 25% SF2	10.16	0.641

Table 5. Chemical and mineralogical composition and loss on ignition of samples SF2 and SF2b

Sample	%Fe	%SiO ₂	%PPC	%Hematite	%Goethite	%Quartz
SF2b	56.81	11.60	6.21	31.90	54.30	10.70
SF2	56.66	11.71	6.12	32.50	53.40	11.30

Table 6. Adjusted coefficient of uniformity for SF2 and TML

Sample	Solids Density d (g/cm ³)	Coefficient of Uniformity	TML (%)
SF2b	4.13	393	13.72
SF2	4.11	151	14.03
SF1	4.34	385	9.10

4 Conclusion

This study identified a positive correlation between goethite content and TML, partially explained by goethite's lower solids density. Notably, higher goethite content coincided with reduced compactness in PFD80 tests, leading to larger voids and further increasing TML. Other properties likely influencing compaction, such as cohesiveness, particle friction, and solid-water interactions, deserve further investigation to clarify the precise mechanisms governing goethite's positive

influence on TML. These findings contribute to a better understanding of TML variability, empowering improved planning of ore products for shipping and more efficient moisture content control practices.

Acknowledgements

The authors are grateful to Vale S/A, CAPES, CNPq and FAPEMIG for all the support provided.

References

- 1 International Maritime Organization – IMO. International Maritime solid bulk cargoes code. London: IMO; 2022.
- 2 Ferreira RF, Pereira TM, Lima RMF. A model for estimating the PFD80 transportable moisture limit of iron ore fines. *Powder Technology*. 2019;345:329-337.
- 3 Ferreira RF. Modelos para previsão do limite de umidade transportável de finos de minério de ferro [thesis]. Ouro Preto: Universidade Federal de Ouro Preto; 2019.
- 4 Ferreira RF, Lima RMF. Relationship between particle size distribution and the PFD80 transportable moisture limit of iron ore fines. *Powder Technology*. 2023;414:118072.
- 5 Ferreira RF, Lima RMF. Influência da massa específica dos sólidos no TML de finos de minério de ferro. In: Associação Brasileira de Metalurgia, Materiais e Mineração. Proceedings of the Proceedings of the 22nd Brazilian Mining Symposium; 2023 Aug. 1-3; São Paulo, Brazil. São Paulo: ABM; 2023.
- 6 Amorim LQ, Alckmim FF. New ore types from the Cauê banded iron-formation, Quadrilátero Ferrífero, Minas Gerais, Brazil - Responses to the growing demand. In: Australasian Institute of Mining and Metallurgy. Proceedings of Iron Ore Conference; 2011 Jul. 11-13; Perth, Austrália. Carlton: AusIMM; 2011.
- 7 Iron Ore Fines Technical Working Group – IOFTWG. Submission for evaluation and verification: terms of reference. London; 2013.
- 8 Iron Ore Fines Technical Working Group – IOFTWG. Submission for evaluation and verification: iron ore Proctor Fagerberg test for iron ore fines. London; 2013.
- 9 Iron Ore Fines Technical Working Group – IOFTWG. Submission for evaluation and verification: marine report. London; 2013.
- 10 Iron Ore Fines Technical Working Group – IOFTWG. Submission for evaluation and verification: reference tests. London; 2013.
- 11 Iron Ore Fines Technical Working Group – IOFTWG. Submission for evaluation and verification: research synopsis and recommendations. London; 2013.
- 12 Minitab LLC. Minitab™ 21.1. 2021 [cited 2023 Jun 30]. Available at: <https://www.minitab.com>
- 13 American Society for Testing and Materials – ASTM. ASTM D5550-14: standard test method for specific gravity of soil solids by gas pycnometer. West Conshohocken: ASTM International; 2014.
- 14 International Organization for Standardization – ISO. ISO 9516-1:2003: iron ores: determination of various elements by X-ray fluorescence spectrometry: part 1: comprehensive procedure. Geneva: ISO; 2003.
- 15 R Core Team. R: a language and environment for statistical computing. Vienna: R Foundation for Statistical Computing; 2022 [cited 2023 Jun 30]. Available at: <http://www.R-project.org/>
- 16 Klein C, Dutrow B. Manual of mineral science. 23rd ed. New York: John Wiley & Sons; 2007.

Received: 25 Jan. 2024

Accepted: 8 July 2024